JOURNAL OF PHYSIOLOGY AND PHARMACOLOGY 2009, 60, 4, 79-84
www.jpp.krakow.pl

A. KALAUZI[1], S. KESIC[2], J. SAPONJIC[2]

CORTICO-PONTINE THETA SYNCHRONIZATION PHASE SHIFT FOLLOWING MONOAMINERGIC LESION IN RAT

[1]Department of Life Sciences, Institute for Multidisciplinary Research, 11000 Belgrade, Serbia; [2]Department of Neurobiology, Institute for Biological Research Sinisa Stankovic, University of Belgrade, 11060, Belgrade, Serbia

The experiments were performed in 14 adult, male Sprague Dawley rats chronically instrumented for sleep recording and recorded during baseline condition, following sham injection (saline i.p. 1 ml/kg), and every week for 5 weeks following injection of the systemic neurotoxins (DSP-4 or PCA; 1 ml/kg, i.p.) for chemical axotomy of the locus coeruleus (LC) and dorsal raphe (DR) axon terminals. In our former study we demonstrated that the systemically induced lesion of the noradrenergic or serotonergic axon terminals did not affect the sleep-wake distribution from control condition. In this study, by using spectral analysis and phase shift spectra of the cortical and pontine EEG we analyzed cortico-pontine theta oscillation synchronization phase shift on 6-hour recordings in control condition and 28 days following the monoaminergic lesions, as a time for permanently established DR or LC chemical axotomy. Our results demonstrated for the first time that chronically decreased brain monoamines in freely moving rats changed cortico-pontine theta synchronization phase shift. Pons became a leading theta oscillator. We assume that deficit of monoamines induced predominance of the NREM/REM transitions, characterized with phasic theta oscillations (the increased density of clustered P waves which intrinsic frequency corresponds to theta frequency oscillations), and may produced preceding phasic theta versus tonic theta oscillation drive.

Key words: *EEG, theta oscillations synchronization, phase shift spectra, cortex, pons, rat, monoaminergic lesion*

INTRODUCTION

There are numerous oscillations in the brain of all species from very slow to very fast, the waking-state related or sleep-related (1-3). Many investigations suggested specific relationship between two or more oscillation bands (4, 5). Neuronal network oscillations in brain function and neuronal synchrony within the same network or between interrelated networks have been extensively and typically investigated on a single oscillation band (6). Still, the exact mechanisms of the most brain oscillations and the mechanisms for the synchronization of neuronal activity within the single brain structure or between different brain structures are not well understood (6). What is generally known so far is that slow oscillators involve larger neuronal areas, whereas higher frequency oscillations are more localized (7).

The hippocampal theta rhythm is the most studied rhythm in rat. Theta oscillations can be coherent across many brain structures, like within the structures of the limbic cortex (8). Theta oscillation is present in the hippocampal and retrohippocampal areas in the cat, rabbit, and human (6, 9). Theta oscillations was considered as a correlate of arousal, orientation, exploration, attention, learning and memory, motivational drives, emotions, voluntary movements, (10), the encoding of new information (11-14).

The origin of the potent ascending multisynaptic brainstem hippocampal synchronizing pathways was originally localized to the rostral pontine region (13). Electrical stimulation of the nucleus reticularis pontis oralis (RPO) (15, 16), and pharmacological stimulation of the pedunculopontine tegmental nucleus (PPT) (17) verified these two pontine structures as the primary brainstem sources for eliciting hippocampal theta field activity. The anatomical tracing studies additionally have verified the reciprocal connectivity between RPO and PPT as well as their efferent projections to subcortical structures involved in theta field generation (13). Ascending brainstem hippocampal synchronizing pathways synapse with several midline diencephalic nuclei which send projections to medial septal region (MS/vDBB), the critical node for further projections to limbic structures such as hippocampal formation, cingulated cortex and entorhinal cortex (9, 13). Increasing level of the ascending brainstem synchronizing activation is translated to hippocampus through the balance of activity of the MS/vDBB cholinergic projections (excitatory drive to hippocampal theta-ON cells) or GABA-ergic projections (inhibition of the hippocampal theta-OFF cells). The ascending brainstem synchronizing pathways influence the electrophysiological and pharmacological properties of the neocortex as well, and functional significance of these pathways is generalized regulation of the neocortical activities related to sensorimotor behavior (13, 15).

It is well known that the pontine cholinergic neurons of the pedunculopontine tegmental nucleus/laterodorsal tegmental nucleus (PPT/LDT), as a part of the ascending brainstem

synchronizing pathway, play crucial role in generation of REM sleep through reciprocal interconnection with serotonergic dorsal raphe (DR) and noradrenergic locus coeruleus (LC) neurons. Inhibitory interaction between these regions are important in regulating their activity (18-21), and reciprocal and opposite discharge patterns of monoaminergic and cholinergic neurons within the pons were proposed to underline the cyclic appearance of REM sleep (21, 22). DR and LC are the main sources of monoamines in the brain. Their extensive efferents implicate these structures in a variety of behavioral functions, particularly in sleep regulation (20, 22), motor and respiratory control (23-25).

Because our former study demonstrated that the systemic selective lesion of the noradrenergic or serotonergic axon terminals did not affect the sleep-wake distribution from control condition (26), in this study, by using spectral analysis and phase shift spectra of the cortical and pontine EEG, we investigated the impact of the monoaminergic lesions on theta oscillations synchronization between sensorimotor cortex and pons.

MATERIALS AND METHODS

The experiments were performed in 14 adult, male Sprague Dawley rats chronically instrumented for sleep recording. The surgical procedures employed for electrode implantation have been previously described (26), and are outlined below. Prior to surgery and consistently throughout the experimental protocol, animals were maintained on a 12 hour light-dark cycle, and were housed at 25°C with free access to food and water. Principles for the care and use of laboratory animals in research were strictly followed, as outlined by the Guide for Care and Use of Laboratory animals (National Academy of Sciences Press, Washington; DC, 1996).

For the operative procedure animals were anesthetized with a combination of 80 mg/kg ketamine (Abbot Laboratories, North Chicago, IL, USA) and 5 mg/kg xylazine (Phoenix Scientific Inc. St. Joseph, MO, USA) by intraperitoneal injection. We implanted bilateral parietal stainless-steel screw electrodes for EEG cortical activity recording (A/P: 2.5; R/L: 2; D/V: 1 to bregma), and a twisted-pair bipolar electrode, fabricated using teflon coated wire (Medwire, Mt. Vernon, NY, USA) with an uninsulated tip of 0.5 mm was stereotaxically targeted into the right PPT (A/P: -7.80; L: 2; D/V: -7.40) for pontine P-wave recording (27), and bilateral electromyogram (EMG) wire electrodes were implanted into the dorsal nuchal musculature to assess skeletal muscle activity. All electrode leads were soldered to a miniature connector plug (39F1401, Newark Electronics, Schaumburg, Illinois, USA), and the assembly was fixed to the screw electrodes and skull using acrylic dental cement (Justi, Saslow Dental, Mt. Prospect, Illinois, USA). Scalp wounds were sutured and the rats were recovered for 2 weeks before experimental recording sessions began. All experimental recordings were bipolar and began at 9:00 a.m. and lasted 6 h. EEG activities carried from the connector plug on the rat head by cable and passed through a sealed port of the plethysmograph were displayed on a computer monitor (Experimenter's Workbench, Datawave Systems, Longmont, CO, USA), and stored on disk for further off-line analysis. After conventional amplification and filtering (0.1-50 Hz band pass; Grass Model 12, West Warwick, RI) the analog data were digitized (sampling frequency 100/s) and recorded using Brain Wave for Windows software (Datawave System Longmont, CO, USA). Each rat was first recorded after saline injection (sham control; saline i.p. 1 ml/kg), and then each week for 5 weeks following injection of a systemic neurotoxin (1 ml/kg, i.p.). We lesioned the dorsal raphe nucleus axon terminals in 7 rats with PCA toxin (p-chloroamphetamine, Sigma-Aldrich, MO) using two intraperitoneal injections (6 mg/kg) 24 h apart (28). Locus coeruleus axon terminals were lesioned in 7 rats using DSP-4 (N-(2-chloroethyl)-N-ethyl-2-bromobenzilamine, Sigma-Aldrich, MO) in a single i.p. injection of 50 mg/kg (29). The neurotoxins were freshly prepared, dissolved in normal saline, and administered in the same volume as the saline sham injection. All procedures for electrodes implantation, lesion induction, and polygraphic recording have been described in detail elsewhere (26). In some animals, we were unable to obtain technically adequate recordings throughout the post-lesion follow-up period (*e.g.* failure of the electrode implant). For analysis of lesion effects in this study, we included only recordings from animals that completed the 5-week post-lesion follow-up period (4 PCA lesioned rats, and 5 DSP-4 lesioned rats).

For the spectral and phase spectra analysis we used overall 6-h recordings in control condition and 28 days following monoaminergic lesions from nine rats. Each lesioned rat was compared in respect to its own control. We extracted all 5 s epochs (4320 epochs of 5 s) from cortical and pontine EEG signals. An example of one 5 s epoch of the analog signals, used for further analysis, in control (A) and lesion condition (B) is depicted on *Fig. 1*. Fourier analysis was performed using standard FFT routine supplied with MATLAB 6.5. Amplitude spectra were calculated for each 5 s epoch and averaged.

In order to calculate theta frequency phase shifts, it is appropriate to treat each of the two signals in this band as amplitude modulated carrier frequency sinusoidal functions:

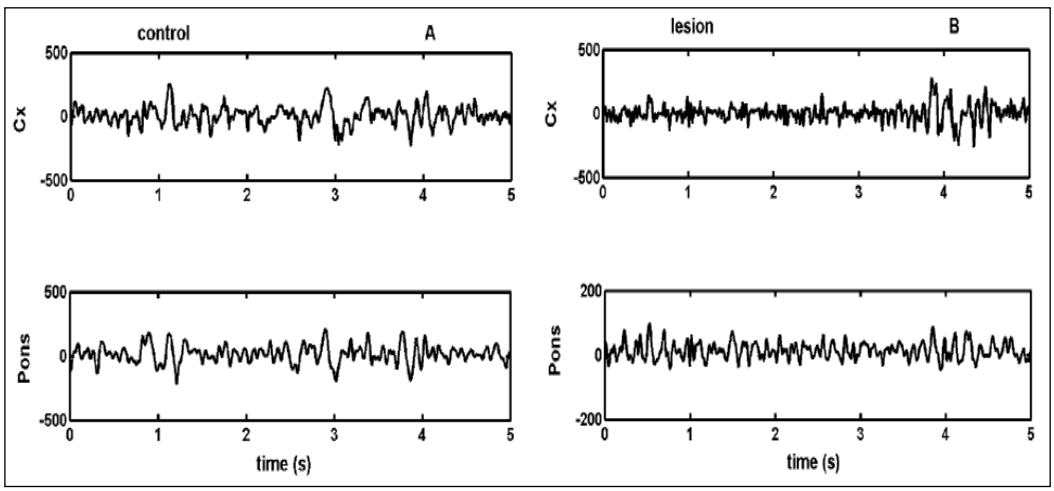

Fig.1. An example of one 5s epoch of analog cortical (Cx) and pontine (Pons) EEG signal in control condition (A) and 28 days following PCA lesion (B).

$$u(t) = \left(1 + u_m(t)\right) A_c \sin(\omega_c t + \varphi_c) \quad (1)$$

where u_m stands for the modulating waveform, while A_c, ω_c and φ_c denote amplitude, circular frequency and initial phase of the carrier sine wave, respectively. If we expand u_m(t) into Fourier series

$$u_m(t) = \sum_{i=1}^{n} U_{mi} \sin(\omega_{mi} t + \varphi_{mi})$$

equation (1) could be rewritten as:

$$u(t) = A_c \sin(\omega_c t + \varphi_c) + \frac{1}{2} A_c \sum_{i=1}^{n} U_{mi} \{\cos[(\omega_c - \omega_{mi})t + \varphi_c - \varphi_{mi}] - \cos[(\omega_c + \omega_m)t + \varphi_c + \varphi_{mi}]\}$$

This equation shows that if the initial phase of the carrier frequency, φ_c, is unknown, it could be assessed by averaging initial phases of Fourier components from the lower and higher side bands of the modulated signal, symmetrically around ω_c, which usually coincides with position of the local band maximum in the amplitude spectrum. Analogously, the same is valid if two signals with variable amplitudes (but equal carrier frequencies) are simultaneously recorded and treated as modulated waveforms; their carrier frequency phase shift $\Delta\varphi_c$ could be obtained by averaging phase shifts of Fourier components, $\Delta\varphi_c \pm \Delta\varphi_{mi}$. Observing the fact that phases and phase differences are angular random variables, amplitude-weighted vector average for calculating $\Delta\varphi_c$ was used:

$$\Delta\varphi_c = \arctan \frac{\sum_{i=1}^{n} A_{1i} A_{2i} \sin(\Delta\varphi_i)}{\sum_{i=1}^{n} A_{1i} A_{2i} \cos(\Delta\varphi_i)}$$

where A_{1i} and A_{2i} stand for amplitudes of the ith Fourier component of the two signals involved (indexed by 1 and 2). A convenient property of this approach is that $\Delta\varphi_c$ does not depend on amplitudes of either of the two signals, consequently there was no need for tracking the degree of amplification or perform calibration.

In our signals, the theta carrier frequency phase shifts (CFPS) were obtained for each epoch of the 4320 epochs by integrating Fourier component phase shifts in the range 4.2–8 Hz according to procedure explained above, and in Kalauzi *et al*. (30), and histogramized. CFPSs for all rats were in the range from 5.2-6.8 Hz. CFPS averages calculated from each histogram were then transformed into corresponding time delays for theta carrier frequency (cf_θ > into→t_D = PS_{av} / (cf_θ x 360°)). The angular sinphasic significances for CFPS, at probability level p, were estimated by comparing values of the detected angular standard deviations (angSD) with probability of their equivalents for random angles (for 4320 epochs the significantly critical, at the level $p<0.05$, was angSD <44,67 deg).

RESULTS

Mean normalized cortical and pontine amplitude spectra of the 6 h recordings depict the characteristic overlapping in the amplitude of theta (5.0–8.0 Hz) band in control condition (*Fig. 2A*, *Fig. 2C*), while their corresponding amplitude spectra 28 days following PCA lesion (*Fig. 2B*) and DSP-4 lesion (*Fig. 2D*) depicted a greater fall of theta amplitudes in the cortical than pontine signals. Determined theta carrier frequencies (cf_θ) for PCA lesioned rats, and for their own controls (n=3/4; six 6-h recordings) were in the range of 6.6-6.8 Hz. The theta carrier frequencies for DSP-4 lesioned rats and for their own controls (n=3/5; six 6-h recordings) were in the range of 5.2-6.6 Hz (*Table 1*). Although there was significant phase-locking between

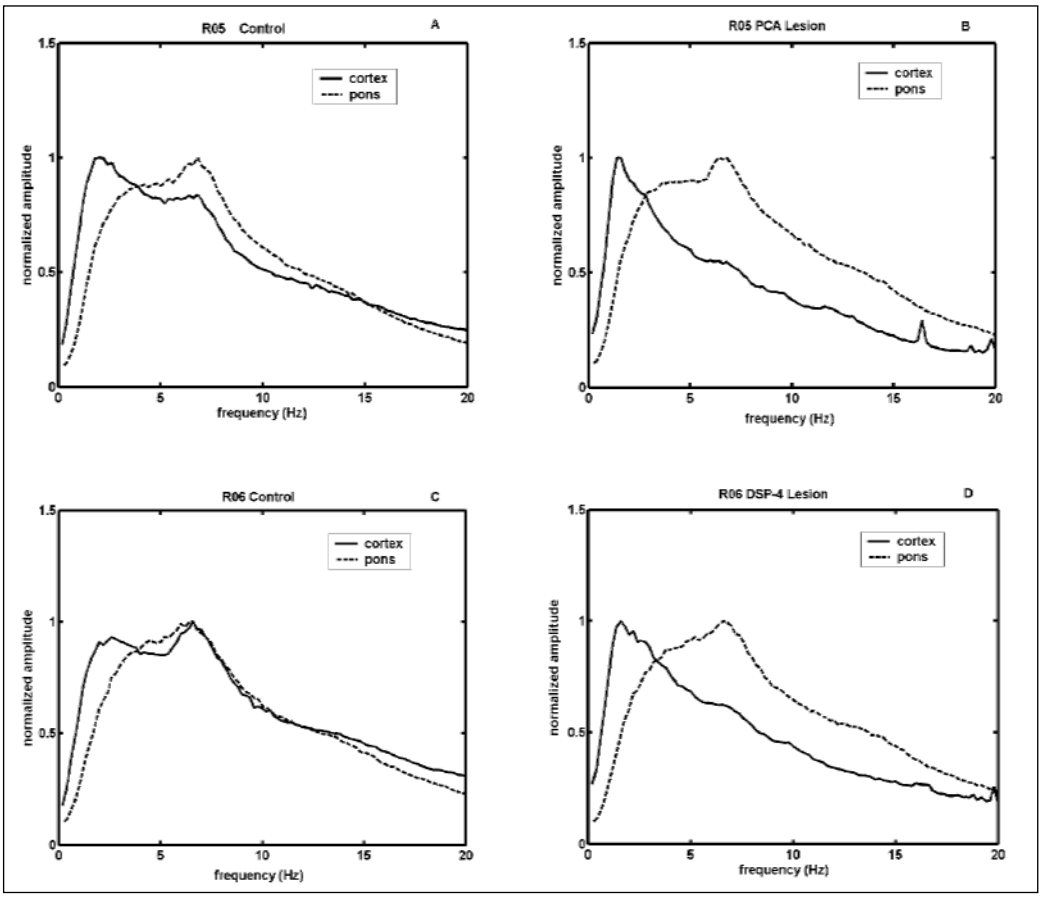

Fig. 2. Mean normalized amplitude spectra of the 6-h recordings (4320 epochs of 5 s per each signal and condition) depict the characteristic overlapping of cortical and pontine spectra in the amplitude of 5-8 Hz band in control condition of two rats (A, C), and their corresponding spectra 28 days after PCA (B) or DSP-4 (D) lesion showed a greater fall of theta amplitudes in the cortical than pontine signals.

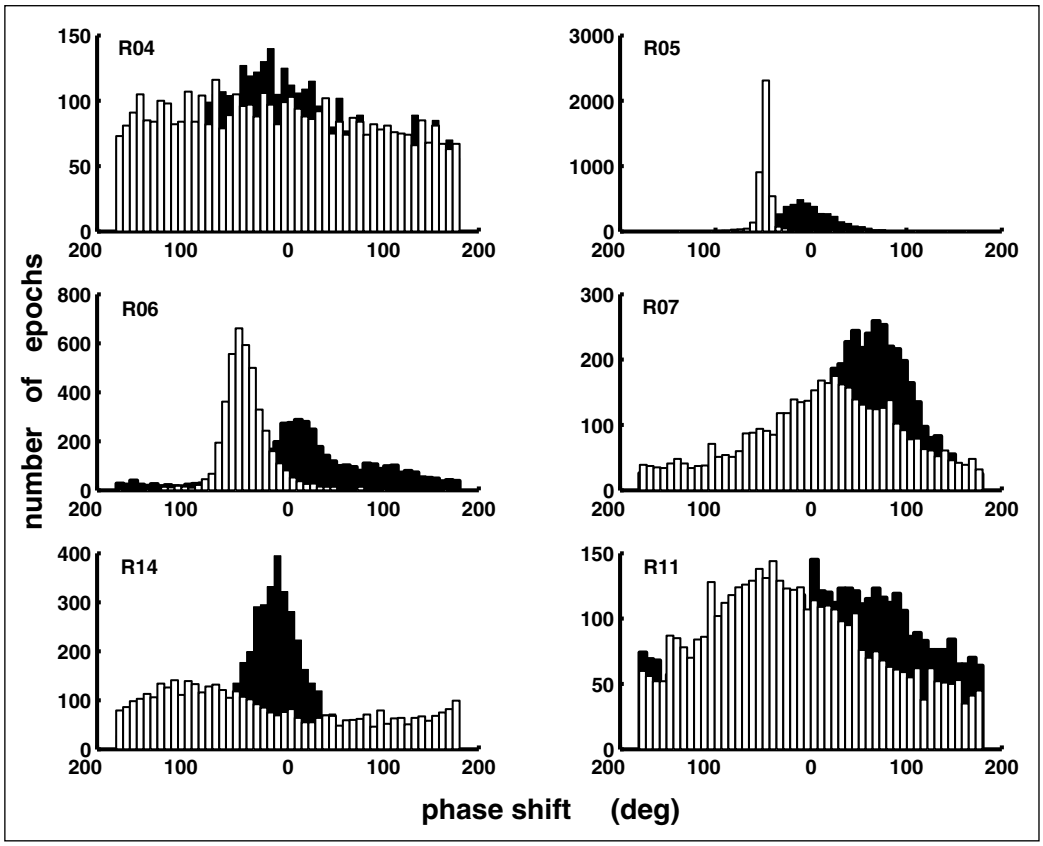

Fig. 3. Histograms of the cortico-pontine theta carrier frequency phase shifts (CFPS) in control condition (black histograms of right and left column) versus 28 days after PCA (white histograms of right column: rat R05, R07, R11) or DSP-4 lesion (white histograms of left column: R04, R06, R14).

Table 1. Lesion induced changes of cortico-pontine theta carrier frequency phase shifts (CFPS) and the corresponding cortico-pontine time delays (t_D) for each rat and each condition: the theta carrier frequencies (cf_θ), the mean values of CFPS (for 4320 epochs of 5 s), their angular standard deviations (angSD) for significance determination at the level $p < 0.05$, the corresponding time delays for each condition and each rat, and cortico-pontine time delays 28 days following lesion versus control condition of each rat.

Rat	cf_θ (Hz)	Control mean CFPS(deg)	Control angSD (deg)	Lesion mean CFPS(deg)	Lesion angSD (deg)	Control t_D (ms)	Lesion t_D (ms)	$\Delta t\theta$ (ms)
R05 (PCA)	6.8	- 4.6	27.5	- 47.8	11.3	- 1.9	- 20.7	18.8
R07 (PCA)	6.8	60.9	37.4	23.3	42.9	24.9	9.5	15.4
R11 (PCA)	6.6	38.9	44.3	- 37.4	44.5	16.4	-15.8	32.2
R04 (DSP-4)	5.2	-21.7	43.3	- 48.8	45.4	-11.6	- 26.1	14.5
R06 (DSP-4)	6.6	28.8	39.6	- 44.3	22.5	12.1	-18.6	30.7
R14 (DSP-4)	6.0	-14.6	32.2	-101.5	43.3	- 6.8	- 47.0	40.2

cortical and pontine theta carrier frequencies during control as well as after monoaminergic lesion in 6/9 rats (*Table 1*; angSD<44.67), in 3/6 control recordings the cortical theta preceded pontine theta, and in 3/6 recordings the pontine theta preceded cortical theta. The histograms of the theta carrier frequency phase shifts of cortical and pontine EEG in control condition (the black histograms on *Fig. 3*), and 28 days following PCA or DSP-4 lesion (the white histograms on *Fig. 3*) have shown the changes in theta oscillation drive. Twenty-eight days following both lesions pons became a leading theta oscillator in all rats except one PCA lesioned rat (*Fig. 3*; 2/4 PCA lesioned rats (right column), and 3/5 DSP-4 lesioned rats (left column)). The lesions induced an increase of the cortico-pontine theta carrier frequency phase shift (*Table 1*). The differences in cortico-pontine theta carrier frequency time delay versus control condition for PCA lesioned rats was from 15.4-32.2 ms, and for DSP-4 rats from 14.5-40.2 ms (*Table 1*). The lesion induced cortico-pontine theta phase shift delay from one rat is presented as a filtered analog signal on *Fig. 4*. Pontine theta precedes the cortical theta.

DISCUSSION

Our results demonstrated for the first time that chronically decreased brain monoamines in freely moving rats changed theta synchronization phase shift between sensorimotor cortical and pontine theta oscillations with respect to control condition. Pons becomes a leading theta oscillator following systemically induced chemical axotomy of the DR and LC efferent system. The obtained results suggest the important role of monoamines in brain theta oscillation synchronization.

It is well known that the hippocampal theta rhythm represents a tonic REM sign (beside activated EEG and muscle atonia), while the ponto-geniculo-occipital waves (PGO waves), or only pontine component of this wave in rat (P wave), is considered as the most

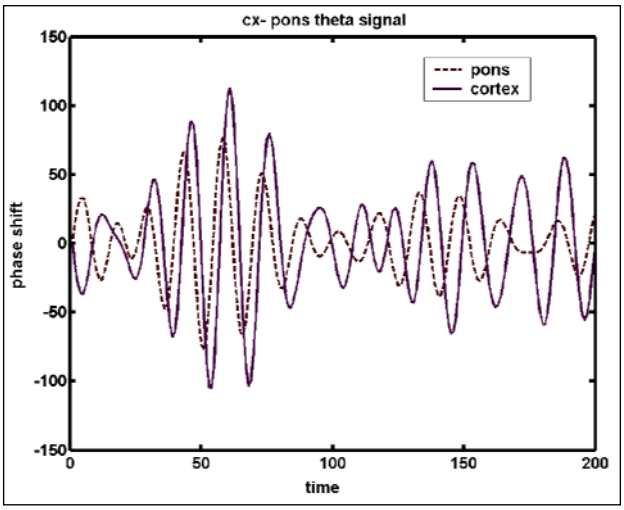

Fig. 4. Cortico (solid line) - pontine (dashed line) theta phase shift presented as filtered analog signal.

prominent electrophysiological REM phasic sign (beside rapid eye movements, muscle twitches, breathing fluctuations, and heart rate surges). PGO/P wave is a field potential as a consequence of phasic activation of a group of neurons in the pontine tegmentum just prior to REM sleep onset, and throughout REM sleep. The PGO/P wave generator is located within the glutamatergic neurons of locus subcoeruleus nucleus within the pons (14, 31), a structure that is widely projected to the PPT (as one of the sources of the ascending brainstem hippocampal synchronizing pathway), hippocampus, amygdala, entorhinal cortex, and visual cortex (31). Anatomical connection between PGO/P wave generator and dorsal hippocampus is also pharmacologically evidenced (32). PGO/P wave activity is positively correlated with hippocampal theta waves during REM sleep (33-35). On the basis of phase-locking between hippocampal theta and PGO/P waves during REM sleep in rats Karashima *et al*. (33) developed three hypotheses: P wave and REM generators control theta frequency and amplitude; theta wave generator controls P wave and REMs densities; and the last hypothesis is that both theta wave dynamics and P wave and REMs densities are controlled by some common mechanisms. On the basis of frequently co-occurring of all phasic events during REM sleep, including PGO/P waves, REM bursts, surges of respiration rhythm and heart rate, and muscle twitches Karashima *et al*. (33) assumed the existence of a common phasic event generator within the brain, and suggested according to other studies (36, 37) the PPT as a possible pontine reticular formation structure that affects the dynamics of the phasic events as well as the hippocampal theta waves. Karashima studies (35) have proved that elicited as well as spontaneous P-waves are phase-locked to the positive hippocampal theta peak.

On the basis of our former study in which we demonstrated that systemically induced monoaminergic lesions failed to produce significant changes in sleep-wake distribution from control condition (26), we investigated in the present study cortico-pontine theta oscillation synchronization phase shift irrespective of state of the animals on overall 6 hour recordings in control condition and 28 days following the monoaminergic lesions (as a time for fully and permanently established DR or LC chemical axotomy). Our results have proved that the tonic deficit of monoamines induced characteristic cortical theta oscillation delay with respect to pons, and pons became the leading theta oscillator. This cortico-pontine theta oscillation "dissociation" caused by monoaminergic lesion could be the reason of the respiratory disturbances simultaneously present in these rats (26, 38). The evidence that intermittent hypoxia induces simultaneous oscillations in the respiratory, cardiovascular and cortical neuronal outputs (39) are in accordance with our results, and suggested also an importance of central nervous system homeostasis for respiratory pattern control.

Here, we assume that deficit of monoamines induced predominance of the NREM/REM transitions, or predominance of the phasic theta oscillations in respect to tonic theta oscillations. The wake/sleep, and specifically NREM/REM transitions are characterized with an increase in P wave densities, particularly clustered P-waves, as already have been defined as the preceding events to REM occurrence. It is well known that intrinsic clustered P wave oscillation frequency corresponds to theta frequency oscillations (14, 31). The increased number of NREM/REM transitions, and an increased density of clustered P-waves caused by monoaminergic deficiency produced preceding phasic theta oscillation drive with respect to tonic theta oscillation drive, or produced pontine theta oscillation leading role.

Acknowledgement: This work was supported by Serbian Ministry of Science and Technological Development Grant No 143005 and 143027, and NIH Grant AG016303.

Conflict of interests: None declared.

REFERENCES

1. Singer W. Synchronization of cortical activity and its putative role in information processing and learning. *Annu Rev Physiol* 1993; 55: 349-374.
2. Buzsaki G. Two-stage model of memory trace formation: a role for 'noisy' states. *Neuroscience* 1989; 1: 551-570.
3. Steriade M. Coherent oscillations and short-term plasticity in corticothalamic networks. *Trends Neurosci* 1999; 22: 337-345.
4. Steriade M, Nunez A, Amzica F. Intracellular analysis of relations between the slow (<1 Hz) neocortical oscillations and other sleep rhythms of the electroencephalogram. *J Neurosci* 1993; 13: 3266-3283.
5. Buzsaki G, Buhl DL, Harris KD, Csicsvari J, Czeh B, Morozov A. Hippocampal network patterns of activity in the mouse. *Neuroscience* 2003; 116: 201-211.
6. Penttonen M, Buzsaki G. Natural logarithmic relationship between brain oscillators. *Thalamus Relat Syst* 2003; 2: 145-152.
7. Contreras D, Llinas R. Voltage-sensitive dye imaging of neocortical spatiotemporal dynamics to afferent activation frequency. *J Neurosci* 2001; 21: 9403-9413.
8. Buzsaki G. Theta oscillations in the hippocampus. *Neuron* 2002; 31: 325-340.
9. Vertes RP, Kocsis B. Brainstem-diencephalo-septohippocampal systems controlling the theta rhythm of the hippocampus. *Neuroscience* 1997; 81: 893-926.
10. Vinogradova OS. Expression, control, and probable functional significance of the neuronal theta-rhythm. *Prog Neurobiol* 1995; 45: 523-583.
11. Klimesch W. EEG alpha and theta oscillations reflect cognitive and memory performance: a review and analysis. *Brain Res Rev* 1999; 29: 169-195.
12. Kahana MJ, Sekuler R, Caplan JB, Kirschen M, Madsen JR. Human theta oscillations exhibit task dependence during virtual maze navigation. *Nature* 1999; 399: 781-784.
13. Bland BH, Oddie SD. Anatomical, electrophysiological and pharmacological studies of ascending brainstem hippocampal synchronizing pathways. *Neurosci Biobehav Rev* 1998; 22: 259-273.
14. Datta S, MacLean RR. Neurobiological mechanisms for the regulation of mammalian sleep-wake behavior:

reinterpretation of historical evidence and inclusion of contemporary cellular and molecular evidence. *Neurosci Biobehav Rev* 2007; 31: 775-824.
15. Vertes RP. Brainstem generation of hippocampal EEG. *Prog Neurobiol* 1982; 19: 159-186.
16. Oddie SD, Bland BH, Colom LV, Vertes RP. The midline posterior hypothalamic region comprises a critical part of the ascending brainstem hippocampal synchronizing pathway. *Hippocampus* 1994; 4: 454-473.
17. Vertes RP, Colom LV, Fortin WJ, Bland BH. Brainstem sites for the carbachol elicitation of the hippocampal theta rhythm in the rat. *Exp Brain Res* 1993; 96: 419-429.
18. McCarley RW, Rainnie GR, Portas DG. Brainstem neuromodulation and REM sleep. *Semin Neurosci* 1995; 7: 341-354.
19. Jones BE. Paradoxical sleep and its chemical/structural substrates in the brain. *Neuroscience* 1991; 40: 637-656.
20. Hobson JA, McCarley RW, Wyzinski PW. Sleep cycle oscillation: reciprocal discharge by two brainstem neuronal groups. *Science* 1975; 189: 55-58.
21. McCarley RW, Hobson JA. Neuronal excitability modulation over the sleep cycle: a structural and mathematical model. *Science* 1975; 189: 58-60.
22. Lydic R, McCarley RW, Hobson JA. Serotonin neurons and sleep. Time course of dorsal raphe discharge, PGO waves, and behavioral states. *Arch Ital Biol* 1987; 126: 1-28.
23. Fenik P, Veasey SC. Pharmacological characterization of serotonergic receptor activity in the hypoglossal nucleus. *Am J Respir Crit Care Med* 2003; 167: 563-569.
24. Carley WD, Radulovacki M. Pathophysiology of sleep-related breathing disorders: unanswered questions. In Sleep-Related Breathing Disorders: Experimental Models and Therapeutic Potential, W.D. Carley, M. Radulovacki (eds). New York, Marcel Dekker Inc., 2003, pp. 3-11.
25. Saponjic J, Cvorovic J, Radulovacki M, Carley DW. Serotonin and noradrenaline modulate respiratory pattern disturbances evoked by glutamate injection into the pedunculopontine tegmentum of anesthetized rats. *Sleep* 2005; 28: 560-570.
26. Saponjic J, Radulovacki M, Carley DW. Monoaminergic system lesions increase post-sigh respiratory pattern disturbance during sleep in rats. *Physiol Behav* 2007; 90: 1-10.
27. Paxinos G., Watson C. The Rat Brain in Stereotaxic Coordinates. San Diego: Academic Press, 1998.
28. Mamounas LA, Molliver ME. Evidence for dual serotonergic projections to neocortex: axons from the dorsal and median raphe nuclei are differentially vulnerable to the neurotoxin p-chloroamphetamine (PCA). *Exp Neurol* 1988; 102: 23-36.
29. Fritschy JM, Grzanna R. Immunohistochemical analysis of the neurotoxic effects of DSP-4 identifies two populations of noradrenergic axon terminals. *Neuroscience* 1989; 30: 181-197.
30. Kalauzi A, Jankovic B, Culic M, Saponjic J, Rajsic N, Suljagic S. Phase demodulation of EEG signals. *Proceedings of the XLII ETRAN Conference* 1998; 4: 204-207.
31. Datta S, Siwek DF, Patterson EH, Cipolloni PB. Localization of pontine PGO wave generation sites and their anatomical projections in the rat. *Synapse* 1998; 30: 409-423.
32. Datta S. Activation of phasic pontine-wave generator: a mechanism for sleep - dependent memory processing. *Sleep Biol Rhythms* 2006; 4: 16-26.
33. Karashima A, Nakao M, Honda K, Iwasaki N, Katayama N, Yamamoto M. Theta wave amplitude and frequency are differentially correlated with pontine waves and rapid eye movements during REM sleep in rats. *Neurosci Res* 2004; 50: 283-289.
34. Karashima A, Nakao M, Katayama N, Honda K. Instantaneous acceleration and amplification of hippocampal theta wave coincident with phasic activities during REM sleep. *Brain Res* 2005; 1051: 50-56.
35. Karashima A, Katayama N, Nakao M. Phase-locking of spontaneous and tone-elicited pontine waves to hippocampal theta waves during REM sleep in rats. *Brain Res* 2007; 1182: 73-81.
36. Datta S, Patterson EH. Activation of phasic pontine wave (P-wave): a mechanism of learning and memory processing. In Sleep and Brain Plasticity. P. Maquet, C. Smith, R. Stickgold (eds). New York, Oxford University Press, 2003, pp. 135-156.
37. Saponjic J, Radulovacki M, Carley DW. P-waves are coupled to long-lasting respiratory disturbance following glutamate stimulation of the pedunculo-pontine tegmental nucleus (PPT). *Sleep* 2003; Suppl. 26: A45-A46.
38. Bojic T, Saponjic J, Radulovacki M, Carley WD, Kalauzi A. Monotone signal segments analysis as a novel method of breath detection and breath-to-breath interval analysis in rat. *Respir Physiol Neurobiol* 2008; 161: 273-280.
39. Budzinska K, Ilasz R. Electroencephalographic and respiratory activities during acute intermittent hypoxia in anesthetized rats. *J Physiol Pharmacol* 2007, 58(Suppl 5): 85-93.

Received: February 16, 2009
Accepted: November 6, 2009-11-09

Author's address: Jasna Saponjic, M.D., Ph.D., Department of Neurobiology, Institute for Biological Research - "Sinisa Stankovic", University of Belgrade, Despot Stefan Bldv. 142, 11060 Belgrade, Serbia; Phone: +381 11 2078426; Fax: +381 11 2761433;
E-mail: jasnasap@ibiss.bg.ac.rs; jasnasaponjic@yahoo.com